Polyvalent Inhibitors Hot Paper

DOI: 10.1002/anie.201400870

Design of Monodisperse and Well-Defined Polypeptide-Based Polyvalent Inhibitors of Anthrax Toxin**

*Sanket Patke, Mohan Boggara, Ronak Maheshwari, Sunit K. Srivastava, Manish Arha, Marc Douaisi, Jacob T. Martin, Ian B. Harvey, Matthew Brier, Tania Rosen, Jeremy Mogridge, and Ravi S. Kane**

Dedicated to Professor George M. Whitesides on the occasion of his 75th birthday

Abstract: *The design of polyvalent molecules, presenting multiple copies of a specific ligand, represents a promising strategy to inhibit pathogens and toxins. The ability to control independently the valency and the spacing between ligands would be valuable for elucidating structure–activity relationships and for designing potent polyvalent molecules. To that end, we designed monodisperse polypeptide-based polyvalent inhibitors of anthrax toxin in which multiple copies of an inhibitory toxin-binding peptide were separated by flexible peptide linkers. By tuning the valency and linker length, we designed polyvalent inhibitors that were over four orders of magnitude more potent than the corresponding monovalent ligands. This strategy for the rational design of monodisperse polyvalent molecules may not only be broadly applicable for the inhibition of toxins and pathogens, but also for controlling the nanoscale organization of cellular receptors to regulate signaling and the fate of stem cells.*

Synthetic polyvalent molecules are currently being developed for applications ranging from pathogen inhibition to drug delivery, the control of cellular signaling, and the inhibition of bacterial toxins.[1–8] Anthrax lethal toxin, which is responsible for the symptoms and mortality of anthrax,[9] is composed of two proteins: lethal factor (LF), an enzyme responsible for host cell death; and protective antigen (PA), which binds to cell-surface receptors and facilitates toxin internalization. Upon binding the host cell, PA is proteolytically processed into a 63 kDa fragment, PA_{63}, which assembles into heptamers, $(PA_{63})_7$, on the surface of the host cell. The binding of the toxic enzyme, LF, to the receptor-bound $(PA_{63})_7$ results in the formation of a complex which is internalized by the host cell (Figure S1). The formation of this complex is one of the key steps in the intoxication pathway (Figure S1B),[10,11] and therapeutics have been designed to inhibit these interactions.[3] In previous work, phage display was used to identify a 12-mer peptide (HTSTYWWLDGAP) that binds to $(PA_{63})_7$.[10] Polyvalent inhibitors have been created by attaching multiple copies of this peptide to a variety of scaffolds such as polymers,[12] liposomes,[13] and β-cyclodextrin.[14]

Structure-based design is a particularly effective strategy to develop polyvalent inhibitors of anthrax lethal toxin and other targets.[11–16] Ligand spacing and valency are key parameters that influence the efficacy of polyvalent molecules (Scheme 1 A).[12–14,17] The ligand spacing is simply the distance separating adjacent ligands on a polyvalent molecule.[5,13,14] Matching the ligand spacing on the polyvalent molecule to the distance between ligand binding sites on the target molecule has been shown to be an effective strategy to design potent polyvalent ligands.[16,18] For a linear polymer or polypeptide, ligand spacing can be manipulated by choosing a linker of appropriate length to separate adjacent ligands on a polyvalent molecule. Optimizing the valency is another effective strategy to enhance the binding of a synthetic polyvalent molecule to its target.[3,5,12–14] For instance, Gujraty et al. designed polyvalent inhibitors of anthrax toxin using polymeric scaffolds of controlled molecular weight and

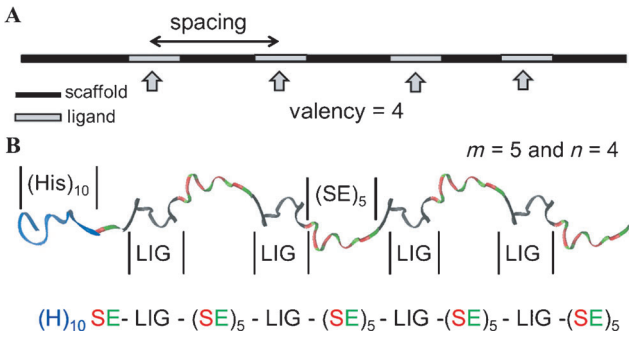

Scheme 1. Controlling the activity of polyvalent molecules. A) Representation showing the key parameters that influence the efficacy of polyvalent molecules—valency and spacing. The valency of the polyvalent molecule depicted is 4. B) Representative image of $(H)_{10}$-SE[LIG-$(SE)_5$]$_4$ polypeptide. Color scheme: black: 12-mer peptide ligand HTSTYWWLDGAP; blue: decahistidine tag; red: serine; green: glutamic acid.

[*] S. Patke, J. T. Martin, M. Brier, T. Rosen, Prof. R. S. Kane
Department of Chemical and Biological Engineering
Rensselaer Polytechnic Institute, Troy, NY 12180 (USA)
E-mail: kaner@rpi.edu
M. Boggara, R. Maheshwari, S. K. Srivastava, M. Arha, M. Douaisi, I. B. Harvey, Prof. R. S. Kane
Center for Biotechnology and Interdisciplinary Studies
Rensselaer Polytechnic Institute, Troy, NY 12180 (USA)
J. Mogridge
Department of Laboratory Medicine and Pathobiology
University of Toronto, Toronto, Ontario, M5S 1A8 (Canada)

[**] This work was supported by NIH grant U01 AI056546, NIH grant R01 EB015482, and the P. K. Lashmet Chair Fund (R.S.K.).

Supporting information for this article is available on the WWW under http://dx.doi.org/10.1002/anie.201400870.

reported an initial sharp increase in potency with increasing valency, followed by a plateau where potency was independent of valency.[12] Matching the valency of the polyvalent molecule to the number of binding sites on the target molecule may also be an effective strategy.[5,12,14]

For polyvalent conjugates, the number of ligand molecules attached to the scaffold can usually be adjusted by varying the relative molar ratio of ligands to scaffold during a conjugation reaction. Bioconjugation coupling strategies such as amine-activated-ester coupling and sulfhydryl–maleimide coupling have been the preferred strategies used to attach multiple copies of ligand molecules to scaffolds.[12,13] However, limited control over the specificity of bioconjugation reactions may result in final products with variation in the number of ligands and position of ligand attachment. As a result, it is difficult to control the final ligand density and ligand spacing precisely and independently. In the case of polymeric scaffolds, the polydispersity of the scaffold may further increase the variability of the polyvalent inhibitor product, which can further complicate characterization efforts. Insufficient control over ligand spacing and valency and scaffold polydispersity are therefore important limitations of some of the typical approaches for designing polyvalent inhibitors.

To address these limitations, we describe an approach to design polyvalent inhibitors of anthrax toxin that are monodisperse and allows for exquisite control over ligand spacing and valency. The ability to make monodisperse biomacromolecular scaffolds by protein-engineering approaches has long been appreciated.[19–23] Kiick and co-workers have used a combination of biosynthetic and chemical approaches to design well-defined polyvalent molecules based on polypeptide scaffolds with different architectures.[24,25] Here we designed polypeptides in which multiple instances of the inhibitory peptide ligand HTSTYWWLDGAP (LIG) were incorporated within the polypeptide sequence in a serial fashion, separated by flexible peptide linker sequences. This biosynthetic approach therefore resulted in polypeptides that were monodisperse and displayed a predefined number of inhibitory peptide instances at defined spacings without the need for a chemical conjugation step. Specifically, we designed monodisperse polypeptides with the sequence $(H)_{10}$-SE[LIG-$(SE)_m]_n$, where the decahistidine tag aids in the purification of the polypeptides, m represents the number of sequential repeats of serine and glutamic acid and therefore controls the ligand spacing, and n represents the number of LIG repeats, i.e. the valency. The polar amino acids serine (S) and glutamic acid (E) were included in the linker sequences to enhance the solubility of the polypeptides. Scheme 1B shows a representation of one such polypeptide sequence for $m = 5$ and $n = 4$.

Thermodynamic models of polyvalent interactions have suggested that the highest avidity of multivalent binding is obtained when the root mean square (RMS) end-to-end length of the linker separating adjacent ligands on a polyvalent molecule matches the separation between the ligand binding sites on the target molecule.[26,27] Therefore we expected that the greatest binding avidity could be obtained if the interligand spacing in the polypeptide inhibitors matched the distance between adjacent binding sites on $(PA_{63})_7$. Our previous work concluded that the 6-mer peptide sequence TYWWLD in the 12-mer peptide HTSTYWWLDGAP was both necessary and sufficient for ligand binding to PA_{63}.[28] In addition, previous mutagenesis studies investigating the interactions between a library of PA mutants and phage presenting the sequence HYTYWWLD had found that the residues P184, L187, K197, and R200 on PA_{63} (indicated by black dots in Scheme 2A and represented by a black rectangular sector symbol in Scheme 2B,C) were important for the binding of the peptide ligand to $(PA_{63})_7$.[14] From the crystal structure of $(PA_{63})_7$,[29] we calculated that the distances between these four amino acid residues on adjacent PA_{63} monomers of $(PA_{63})_7$ were in the 25–35 Å range (Table S1 and Scheme 2A). Assuming that the binding of the divalent $(H)_{10}$-SE[LIG$(SE)_m]_2$ polypeptides to two adjacent PA_{63} monomers of $(PA_{63})_7$ (Scheme 2C) occurs primarily through the interactions between the 6-mer TYWWLD sequence and the predicted ligand binding site on PA_{63}, the sequence GAP-$(SE)_m$-HTS serves as the linker separating adjacent ligands on the polypeptide. Based on thermodynamic models, enhanced divalent binding could be expected if the root mean square (RMS) end-to-end distance of the GAP-$(SE)_m$-HTS polypeptide sequence was also in the range of 25–35 Å. Linkers with RMS end-to-end distances in this range might be obtained by choosing appropriate values of m.

We performed replica exchange molecular dynamics (REMD) simulations to guide our choice of optimal values for m. Conformational sampling studies were performed using implicit solvent REMD simulations to predict the range of conformations that GAP-$(SE)_m$-HTS linkers can assume for different values of m. As shown in Table S2, these studies suggested that GAP-$(SE)_m$-HTS linkers with $m = 5$–7 would have RMS end-to-end distances in the desired range of 25–35 Å. Therefore, we hypothesized that linkers with $m = 5$–7 would enhance the polyvalent binding of the polypeptides to $(PA_{63})_7$ and correspondingly increase the inhibitory efficacy.

Next, we performed experiments to test the validity of the simulation predictions and to study the effect of ligand spacing (m) and valency (n) on inhibitory potency. To

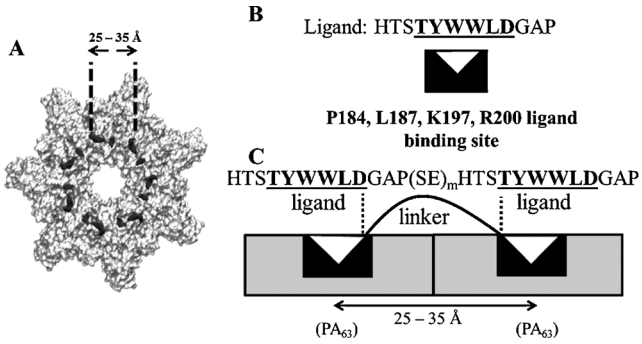

Scheme 2. Representation of binding of the polypeptide-based inhibitors to adjacent sites on $(PA_{63})_7$. A) Structure of $(PA_{63})_7$ with black dots on individual PA_{63} monomers representing the predicted binding sites (P184, L187, K197, and R200) for the 12-mer ligand. B) Representation showing the interaction of the 6-mer TYWWLD (white triangle) with its binding site on PA_{63} (black sector symbol). C) Representation of interactions between a divalent polypeptide and binding sites on adjacent PA_{63} monomers of $(PA_{63})_7$.

characterize the effect of ligand spacing, we determined the ability of divalent polypeptides ($(H)_{10}$-SE[LIG$(SE)_m]_2$) with $m = 3$–13 to inhibit anthrax lethal toxin in a cytotoxicity assay. The procedures used for the generation of plasmids encoding the polypeptide sequences (Figure S2) and for polypeptide expression and purification have been described in detail in the Supporting Information. Half-maximal inhibitory potency (IC_{50}) values for the polypeptide inhibitors were determined using the dose–response curves for individual polypeptides and expressed on a per-peptide basis (Figure 1). As shown in Figure 1 A, all $(H)_{10}$-SE[LIG$(SE)_m]_2$ polypeptides ($m = 3$–13) exhibited submicromolar IC_{50} values; polypeptides with values of m ranging from 5 to 13 exhibited the lowest IC_{50} values (ca. 60–90 nM). These results are consistent with the results from our REMD simulations (see above). Based on these results we selected $m = 5$ because it corresponded to the minimum linker length required for a divalent polypeptide to exhibit maximum inhibition of anthrax lethal toxin.

We next performed cytotoxicity experiments to determine the effect of valency (i.e., the value of n) on the inhibitory potency. To that end, we expressed, purified, and assayed polypeptides of the form $(H)_{10}$-SE[LIG$(SE)_5]_n$ with $n = 2$–9. As shown in Figure 1 B, we found that the IC_{50} values of the polypeptides decreased with an increase in valency. The IC_{50} values for polypeptides with $n = 7$, 8, and 9 were very similar and were in the 2–5 nM range. Based on these results we chose the inhibitor with $n = 7$ for further characterization and optimization because it achieved the maximum inhibition of anthrax toxin with the minimum number of ligands and our selected interligand spacing.

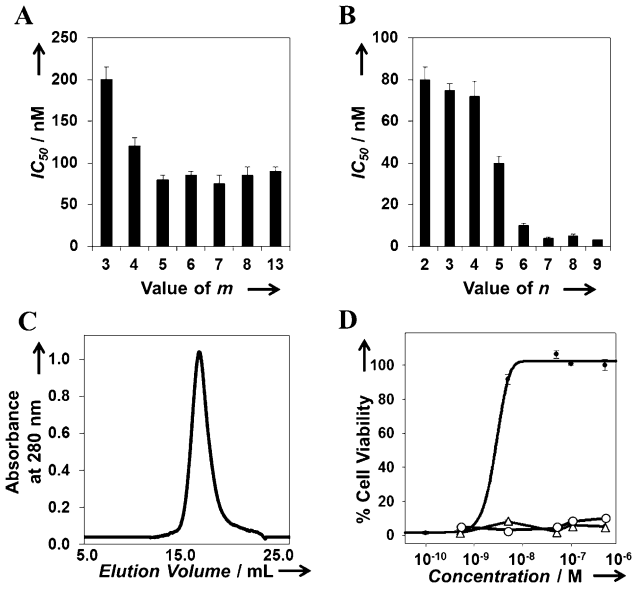

Figure 1. A) Influence of ligand spacing on the inhibitory potency of polypeptide inhibitors of the form $(H)_{10}$-SE[LIG$(SE)_m]_2$. Estimates of the corresponding RMS linker lengths can be found in Table S2 in the Supporting Information. B) Influence of valency on the inhibitory potency of polypeptide inhibitors of the form $(H)_{10}$-SE[LIG$(SE)_5]_n$. C) SEC elution profile of $(H)_{10}$-SE[LIG$(SE)_5]_7$ polypeptide inhibitor. D) Comparison of dose–response curves for $(H)_{10}$-SE[LIG$(SE)_5]_7$ (line with black circles), Ac-HTSTYWWLDGAPK-Am inhibitory peptide (line with white triangles), and negative control $(H)_{10}$-SE[CTRL$(SE)_5]_7$ polypeptide (line with white circles).

Characterization by size-exclusion chromatography indicated that the selected polypeptide, $(H)_{10}$-SE[LIG$(SE)_5]_7$, eluted as a single peak, suggesting that it was monodisperse (Figure 1 C). Secondary-structure characterization by far-UV circular dichroism (CD) spectroscopy indicated that the candidate polypeptide inhibitor was rich in random-coil content, suggesting that the polypeptide was flexible (data not shown). Figure 1 D compares the dose–response curves for $(H)_{10}$-SE[LIG$(SE)_5]_7$, the monovalent Ac-HTSTYWWLDGAPK-Am inhibitory peptide, and a control polypeptide $(H)_{10}$-SE[CTRL$(SE)_5]_7$, where the HTSTYWWLDGAP inhibitory peptide region was replaced by the sequence HTSGGGSGGGAP (CTRL), lacking the PA_{63}-binding TYWWLD sequence. Cytotoxicity assays indicated negligible inhibitory activity against anthrax lethal toxin for the monovalent peptide and the polypeptide control (Figure 1 D). The IC_{50} value of the candidate polypeptide $(H)_{10}$-SE[LIG$(SE)_5]_7$, (4 ± 0.5) nM on a per-peptide basis, was more than four orders of magnitude lower than that for the monovalent peptide, which showed negligible inhibitory activity even at concentrations as high as 100 μM.[10]

While an in vivo characterization of the inhibitors is beyond the scope of the current study, we proceeded to characterize and optimize their serum stability, which will be critical for the successful use of polypeptide-based inhibitors in vivo. To test whether the candidate polypeptide was resistant to proteolytic degradation, we performed serum stability studies as described previously.[14] The candidate polypeptide was incubated in 80% mouse serum at 37 °C. Samples were removed at various time intervals and their inhibitory activity was determined using the cytotoxicity assay. As shown in Figure 2 A, samples incubated in serum for 24 and 48 h failed to exhibit any inhibitory activity in RAW264.7 cells after exposure to anthrax lethal toxin even at inhibitor doses as high as 1 μM.

We explored PEGylation as an approach to improve the serum stability of the candidate polypeptides, since this strategy has been shown to be effective in several previous reports.[30] To that end, we first used site-directed mutagenesis to replace the N-terminal histidine with a cysteine residue, and expressed and purified the resulting polypeptide ($C(H)_9$-SE[LIG$(SE)_5]_7$). As shown in Figure 2 B, introduction of a cysteine at the N-terminus did not have a significant effect on the inhibitory potency, with $C(H)_9$-SE[LIG$(SE)_5]_7$ and $(H)_{10}$-SE[LIG$(SE)_5]_7$ exhibiting IC_{50} values of (4 ± 1) nM and (3 ± 0.7) nM, respectively. Next, we PEGylated $C(H)_9$-SE-[LIG$(SE)_5]_7$ using methoxy-PEG-maleimide in a procedure described in the Supporting Information. 20 kDa PEGs were conjugated to $C(H)_9$-SE[LIG$(SE)_5]_7$ to yield PEG20k-$C(H)_9$-SE[LIG$(SE)_5]_7$. PEGylated polypeptides were separated from non-PEGylated polypeptides and unreacted PEG molecules using size-exclusion chromatography. The IC_{50} value of PEG20k-$C(H)_9$-SE[LIG$(SE)_5]_7$ was (9 ± 1.2) nM (Figure 2 B), indicating that PEGylation did not significantly disrupt the activity of the candidate polypeptide.

Next, we tested the effect of PEGylation on the serum stability of the candidate polypeptide. While incubation of $(H)_{10}$-SE[LIG$(SE)_5]_7$ in serum for 24 h resulted in the loss of its ability to inhibit anthrax lethal toxin (Figure 2 A), serum-

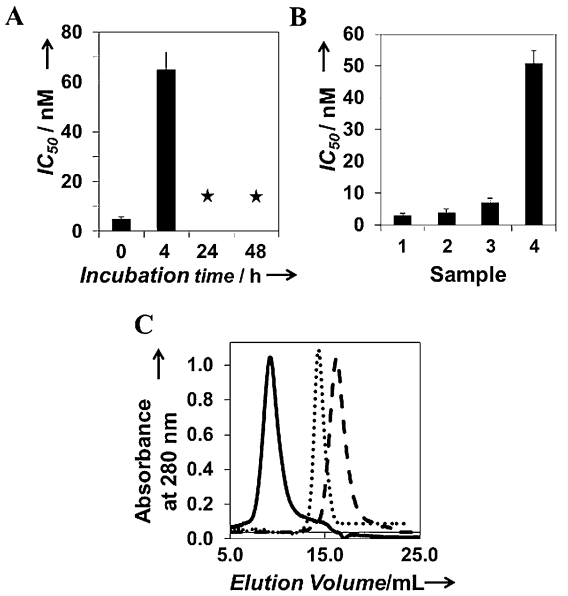

Figure 2. Effect of PEGylation on serum stability, activity, and hydrodynamic radius of $(H)_{10}$-SE[LIG$(SE)_5]_7$. A) Serum stability of $(H)_{10}$-SE[LIG$(SE)_5]_7$. B) Effect of PEGylation on inhibitory potency. IC_{50} values for $(H)_{10}$-SE[LIG$(SE)_5]_7$ (1), C$(H)_9$-SE[LIG$(SE)_5]_7$ (2), PEG20k-C$(H)_9$-SE-[LIG$(SE)_5]_7$ (3), and PEG20k-C$(H)_9$-SE[LIG$(SE)_5]_7$ (4) after incubation in 80% mouse serum for 24 h. C) SEC elution profiles of $(H)_{10}$-SE-[LIG$(SE)_5]_7$ (dashed line), bovine serum albumin (dotted line), and PEG20k-C$(H)_9$-SE[LIG$(SE)_5]_7$ (black solid line). The maximum dose tested in (A) and (B) was 1 μM on a per-peptide basis. Black stars in (A) indicate that inhibitory activity was not detected.

incubated PEG20k-C$(H)_9$-SE[LIG$(SE)_5]_7$ successfully neutralized anthrax lethal toxin with an IC_{50} value of (51 ± 4) nM (Figure 2B). These results suggest that a balance between inhibitory potency and serum stability can be obtained by PEGylating the candidate polypeptides with 20 kDa PEG. Moreover, characterization by SEC indicated that PEG20k-C$(H)_9$-SE[LIG$(SE)_5]_7$ ($M_w \approx 39$ kDa) eluted earlier than bovine serum albumin (BSA) (Figure 2C), indicating that it had a larger hydrodynamic radius than BSA. This result suggests that PEGylation of the polypeptide inhibitors may not only improve their serum stability but also their blood residence time, since proteins with a hydrodynamic radius equal to or greater than that of BSA are expected to have enhanced kidney retention and higher half-life in vivo.[31]

In conclusion, we have demonstrated the structure-based design of potent polyvalent inhibitors of anthrax lethal toxin. This protein-engineering approach provides the requisite control over both ligand spacing and valency that is critical for elucidating structure–activity relationships. This strategy for the rational design of monodisperse polyvalent molecules could be broadly applicable not only for the inhibition of toxins and pathogens but also for the control of receptor clustering and cellular signaling in vitro and in vivo.[1,3,6–8]

Received: January 27, 2014
Published online: April 6, 2014

Keywords: anthrax toxin · multivalency · periodic polypeptides · protein engineering · structure–activity relationships

[1] M. Mammen, S. K. Choi, G. M. Whitesides, *Angew. Chem.* **1998**, *110*, 2908 – 2953; *Angew. Chem. Int. Ed.* **1998**, *37*, 2754 – 2794.
[2] V. M. Krishnamurthy, L. A. Estroff, G. M. Whitesides in *Fragment-based approaches in drug discovery*, Wiley-VCH, Weinheim, **2006**, pp. 11 – 53.
[3] D. Vance, M. Shah, A. Joshi, R. S. Kane, *Biotechnol. Bioeng.* **2008**, *101*, 429 – 434.
[4] D. R. Bundle, P. I. Kitov, J. M. Sadowska, G. Mulvey, G. D. Armstrong, H. Ling, N. S. Pannu, R. J. Read, *Nature* **2000**, *403*, 669 – 672.
[5] E. K. Fan, E. A. Merritt, C. L. M. J. Verlinde, W. G. J. Hol, *Curr. Opin. Struct. Biol.* **2000**, *10*, 680 – 686.
[6] G. Maheshwari, G. Brown, D. A. Lauffenburger, A. Wells, L. G. Griffith, *J. Cell Sci.* **2000**, *113*, 1677 – 1686.
[7] L. L. Kiessling, J. E. Gestwicki, L. E. Strong, *Angew. Chem.* **2006**, *118*, 2408 – 2429; *Angew. Chem. Int. Ed.* **2006**, *45*, 2348 – 2368.
[8] A. Conway, T. Vazin, D. P. Spelke, N. A. Rode, K. E. Healy, R. S. Kane, D. V. Schaffer, *Nat. Nanotechnol.* **2013**, *8*, 831 – 838.
[9] R. J. Collier, J. A. T. Young, *Annu. Rev. Cell Dev. Biol.* **2003**, *19*, 45 – 70.
[10] M. Mourez, R. S. Kane, J. Mogridge, S. Metallo, P. Deschatelets, B. R. Sellman, G. M. Whitesides, R. J. Collier, *Nat. Biotechnol.* **2001**, *19*, 958 – 961.
[11] E. M. Nestorovich, S. M. Bezrukov, *Chem. Rev.* **2012**, *112*, 6388 – 6430.
[12] K. V. Gujraty, A. Joshi, A. Saraph, V. Poon, J. Mogridge, R. S. Kane, *Biomacromolecules* **2006**, *7*, 2082 – 2085.
[13] P. Rai, C. Padala, V. Poon, A. Saraph, S. Basha, S. Kate, K. Tao, J. Mogridge, R. S. Kane, *Nat. Biotechnol.* **2006**, *24*, 582 – 586.
[14] A. Joshi, S. Kate, V. Poon, D. Mondal, M. B. Boggara, A. Saraph, J. T. Martin, R. McAlpine, R. Day, A. E. Garcia, J. Mogridge, R. S. Kane, *Biomacromolecules* **2011**, *12*, 791 – 796.
[15] L. L. Kiessling, L. E. Strong, J. E. Gestwicki, *Annu. Rep. Med. Chem.* **2000**, *35*, 321 – 330.
[16] B. D. Polizzotti, R. Maheshwari, J. Vinkenborg, K. L. Kiick, *Macromolecules* **2007**, *40*, 7103 – 7110.
[17] R. Maheshwari, E. A. Levenson, K. L. Kiick, *Macromol. Biosci.* **2010**, *10*, 68 – 81.
[18] S. Mallik, S. D. Plunkett, P. K. Dhal, R. D. Johnson, D. Pack, D. Shnek, F. H. Arnold, *New J. Chem.* **1994**, *18*, 299 – 304.
[19] S. A. Maskarinec, D. A. Tirrell, *Curr. Opin. Biotechnol.* **2005**, *16*, 422 – 426.
[20] Y. L. Boersma, A. Plückthun, *Curr. Opin. Biotechnol.* **2011**, *22*, 849 – 857.
[21] N. E. Davis, L. S. Karfeld-Sulzer, S. Ding, A. E. Barron, *Biomacromolecules* **2009**, *10*, 1125 – 1134.
[22] J. Yang, I. Gitlin, V. M. Krishnamurthy, J. A. Vazquez, C. E. Costello, G. M. Whitesides, *J. Am. Chem. Soc.* **2003**, *125*, 12392 – 12393.
[23] M. Amiram, F. G. Quiroz, D. J. Callahan, A. Chilkoti, *Nat. Mater.* **2011**, *10*, 141 – 148.
[24] Y. Wang, K. L. Kiick, *J. Am. Chem. Soc.* **2005**, *127*, 16392 – 16393.
[25] A. Top, K. L. Kiick, *Adv. Drug Delivery Rev.* **2010**, *62*, 1530 – 1540.
[26] J. M. Gargano, T. Ngo, J. Y. Kim, D. W. K. Acheson, W. J. Lees, *J. Am. Chem. Soc.* **2001**, *123*, 12909 – 12910.
[27] R. S. Kane, *Langmuir* **2010**, *26*, 8636 – 8640.
[28] K. Gujraty, S. Sadacharan, M. Frost, V. Poon, R. S. Kane, J. Mogridge, *Mol. Pharm.* **2005**, *2*, 367 – 372.
[29] C. Petosa, R. J. Collier, K. R. Klimpel, S. H. Leppla, R. C. Liddington, *Nature* **1997**, *385*, 833 – 838.
[30] G. Pasut, F. M. Veronese, *Drugs Today* **2009**, *45*, 687 – 695.
[31] M. J. Knauf, D. P. Bell, P. Hirtzer, Z. P. Luo, J. D. Young, N. V. Katre, *J. Biol. Chem.* **1988**, *263*, 15064 – 15070.

